Energy Materials

**Supplementary Materials**

# $Fe^{3+}$-driven tunnel engineering for stabilizing metastable ramsdellite $MnO_2$ in high-performance zinc-ion batteries

**Yutong Meng[1], Yangfan Li[1], Hang Xiao[1], Xiang Wang[1], Zhiwen Wang[1], Fan Zhang[2,*], Wenqing Ma[3], Da Xiong[1], Zisheng Xiao[1,*], Jiang Yin[1], Zhiye Yuan[4], Tong Zhou[4], Lishan Yang[1,*], Changhui Liu[5], Xiongwei Wu[1]**

[1]Key Laboratory of Chemical Biology & Traditional Chinese Medicine Research (Ministry of Education of China), National and Local Joint Engineering Laboratory for New Petrochemical Materials and Fine Utilization of Resources, Key Laboratory of the Assembly and Application of Organic Functional Molecules of Hunan Province, Key Laboratory of Light Energy Conversion Materials of Hunan Province, Hunan Normal University, Changsha 410081, Hunan, China.
[2]College of Chemistry and Chemical Engineering, Central South University, Changsha 410083, Hunan, China.
[3]Institute for Advanced Interdisciplinary Research (iAIR), Collaborative Innovation Center of Technology and Equipment for Biological Diagnosis and Therapy in Universities of Shandong, School of Chemistry and Chemical Engineering, University of Jinan, Jinan 250022, Shandong, China.
[4]Xiangtan Electrochemical Technology Co., Ltd, Xiangtan 411100, Hunan, China.
[5]College of Chemistry and Chemical Engineering, Hunan Institute of Science and Technology, Yueyang, 414006, Hunan, China.

[*]**Correspondence to:** Prof. Lishan Yang and Dr. Zisheng Xiao, College of Chemistry and Chemical Engineering, Hunan Normal University, No.036 Lushan Road, Changsha 410081, Hunan, China. E-mail: lsyang@hunnu.edu.cn; zishengxiao@hunnu.edu.cn; Dr. Fan Zhang, College of Chemistry and Chemical Engineering, Central South University, No.932 South Lushan Road, Changsha 410083, Hunan, China. E-mail: 242301028@csu.edu.cn

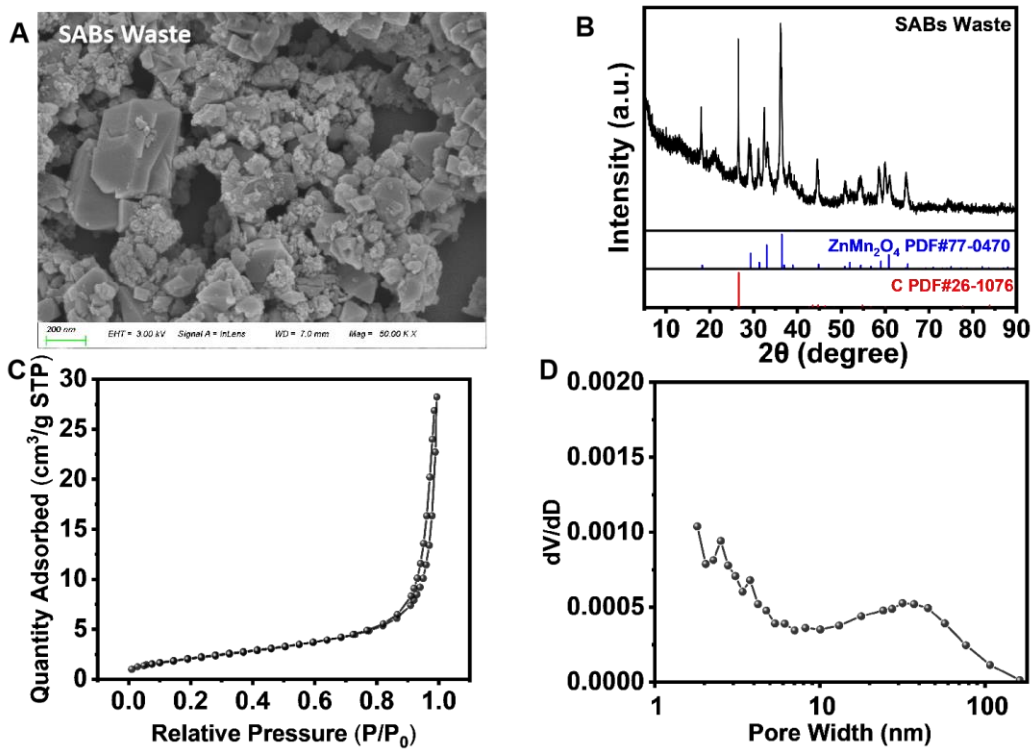


**Supplementary Figure 1.** Basic test of the SABs (A) SEM image. (B) XRD pattern. (C-D) $N_2$ adsorption/desorption isotherm and corresponding pore size distribution.

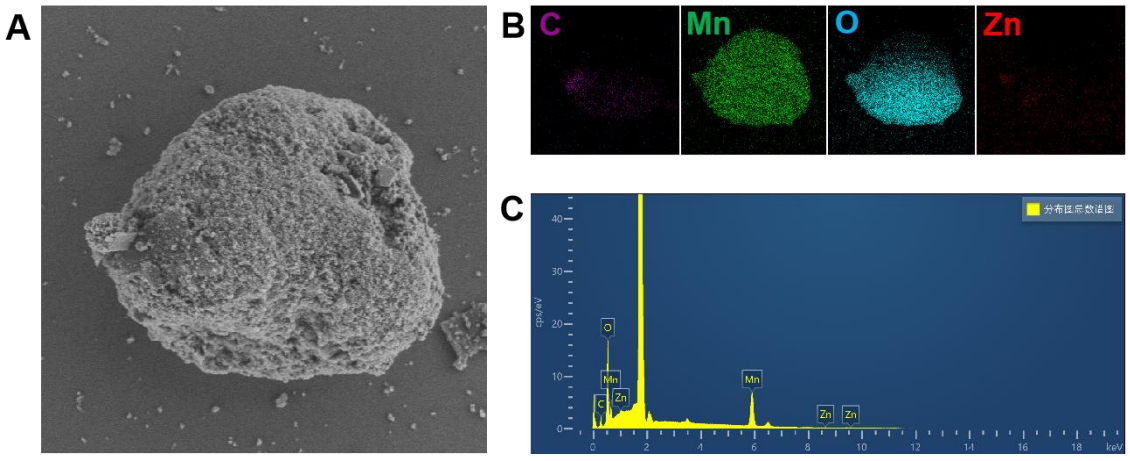


**Supplementary Figure 2.** SEM images after alkali and acid treatment of the SABs (A) SEM image. (B) EDS-Mapping. (C) Element content.

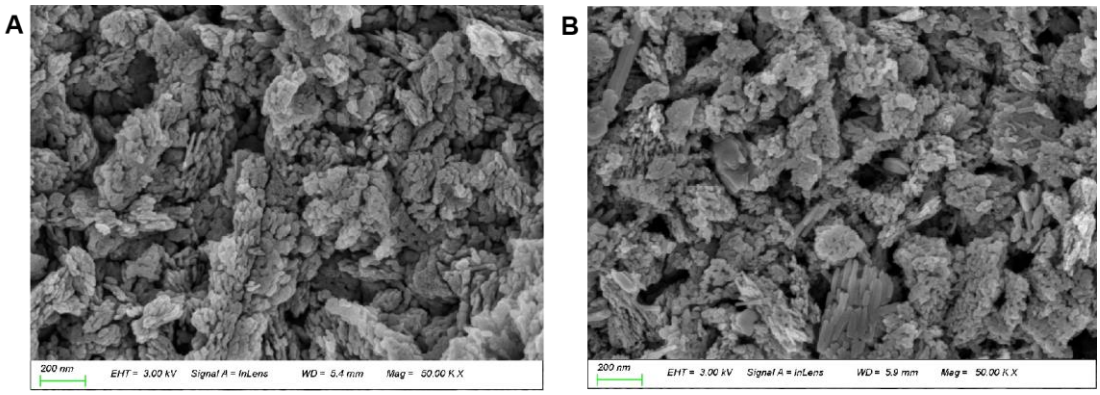


**Supplementary Figure 3.** SEM images of (A) Mn:Fe=100:2 feed ratio. (B) Mn:Fe=100:10 feed ratio.

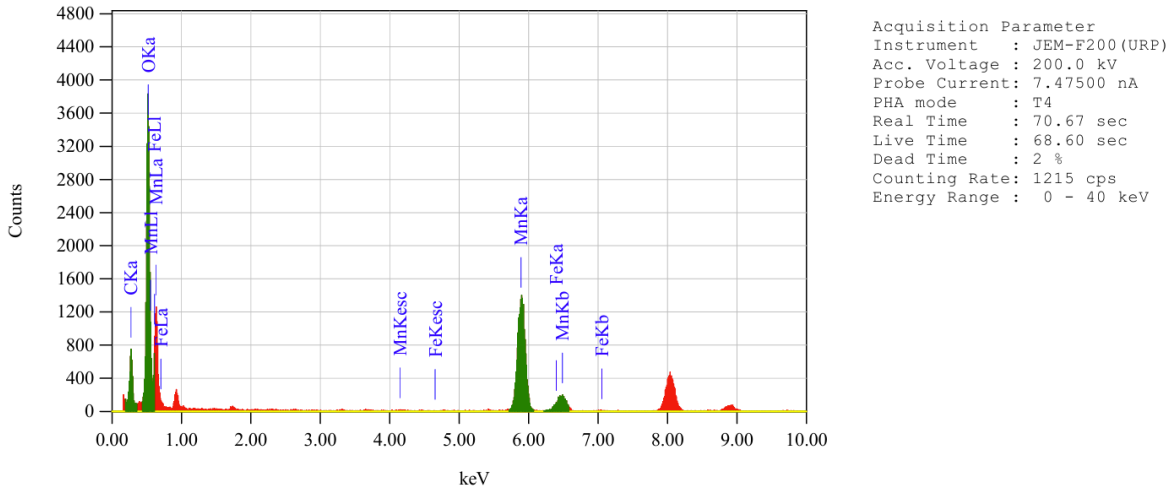


Thin Film Standardless Standardless Quantitative Analysis
Fitting Coefficient : 0.1755

| Element | (keV) | Mass% | Counts | Sigma | Atom% | Compound | Mass% | Cation | K |
|---|---|---|---|---|---|---|---|---|---|
| C K | 0.277 | 16.72 | 3110.25 | 0.23 | 28.39 | | | | 2.3594 |
| O K (Ref.) | 0.525 | 45.03 | 19764.23 | 0.40 | 57.41 | | | | 1.0000 |
| Mn K | 5.894 | 37.10 | 18535.12 | 0.44 | 13.78 | | | | 0.8786 |
| Fe K | 6.398 | 1.15 | 553.99 | 0.09 | 0.42 | | | | 0.9143 |
| Total | | 100.00 | | | 100.00 | | | | |

**Supplementary Figure 4.** Corresponding EDX energy dispersive spectrum of *R*-$Fe_xMn_{1-x}O_2$.

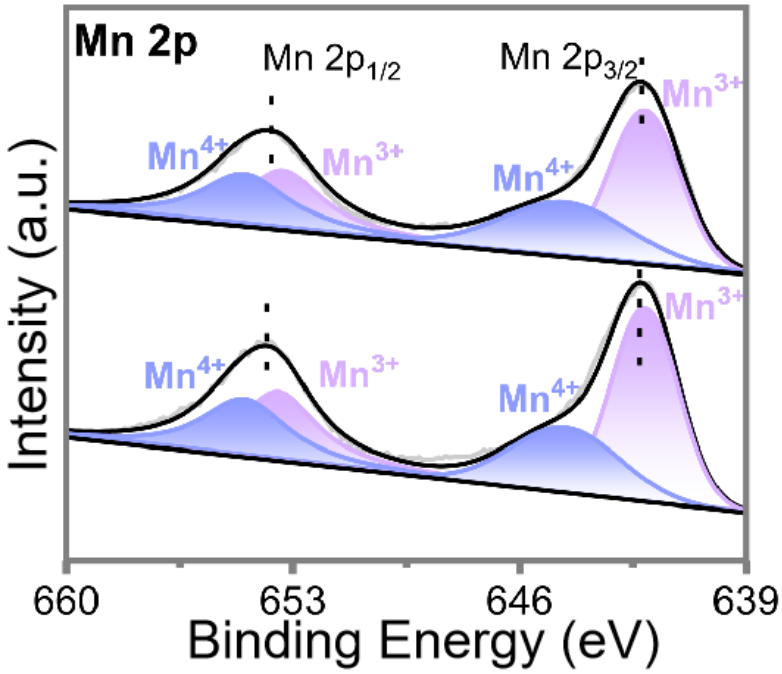


**Supplementary Figure 5.** Mn 2p XPS spectra of $\beta$-$MnO_2$ and $R$-$Fe_xMn_{1-x}O_2$.

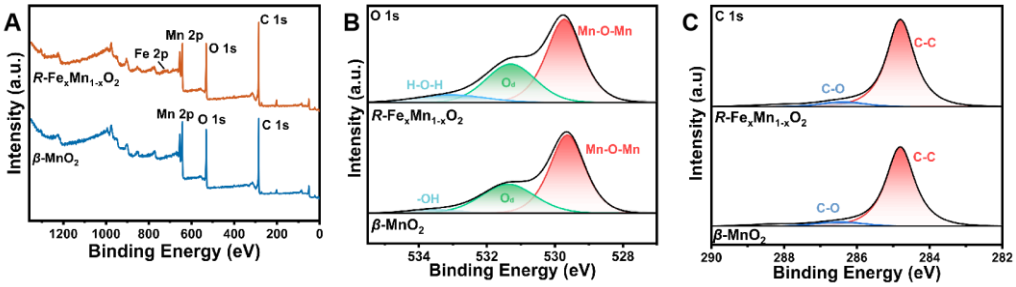


**Supplementary Figure 6.** (A) XPS survey spectra of the two samples ($\beta$-$MnO_2$ and $R$-$Fe_xMn_{1-x}O_2$). (B) O 1s XPS spectra of the two samples. (C) C 1s XPS spectra of two samples.

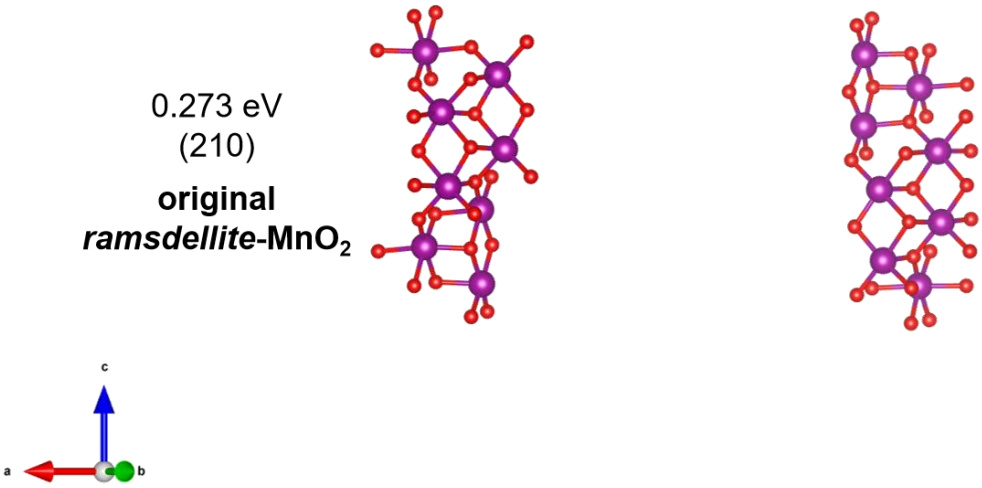


**Supplementary Figure 7.** Surface structure and surface energy of the pristine surface of original *R*-$MnO_2$**.**

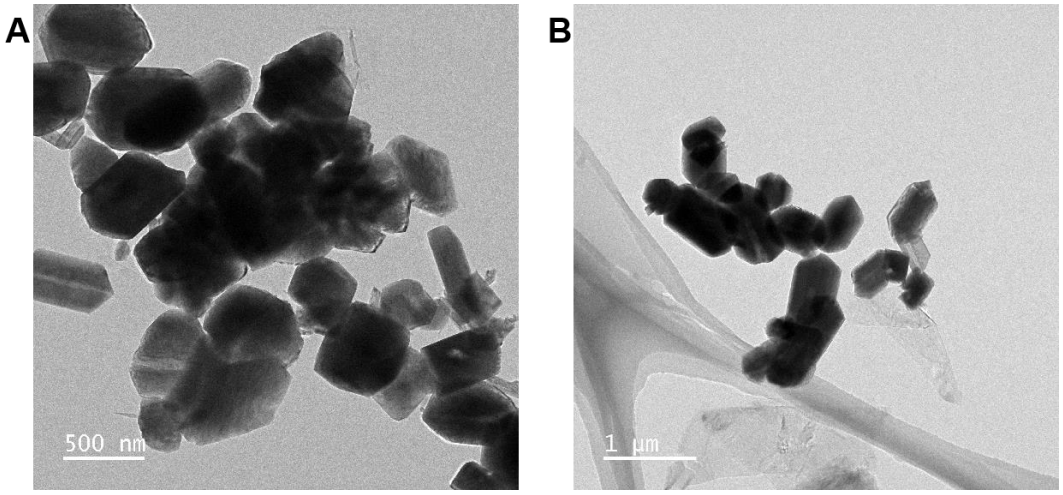


**Supplementary Figure 8.** TEM images of the *β*-$MnO_2$ materials.

To systematically investigate the electrochemical modulation induced by $Fe^{3+}$ doping, controlled synthesis protocols were implemented with varying nominal Fe:Mn ratios: *R*-$Fe_xMn_{1-x}O_2$-1 (nominal 2:100 Fe:Mn atomic ratio); *R*-$Fe_xMn_{1-x}O_2$-2 (nominal 5:100 Fe:Mn atomic ratio); *R*-$Fe_xMn_{1-x}O_2$-3 (nominal 10:100 Fe:Mn atomic ratio), ensuring precise stoichiometric control during hydrothermal synthesis. Notably, the *R*-$Fe_xMn_{1-x}O_2$ designation defaults to the Fe:Mn=100:5 variant unless otherwise specified. This parametric design enables comparative analysis of dopant concentration effects on (de)intercalation thermodynamics and phase stability evolution.

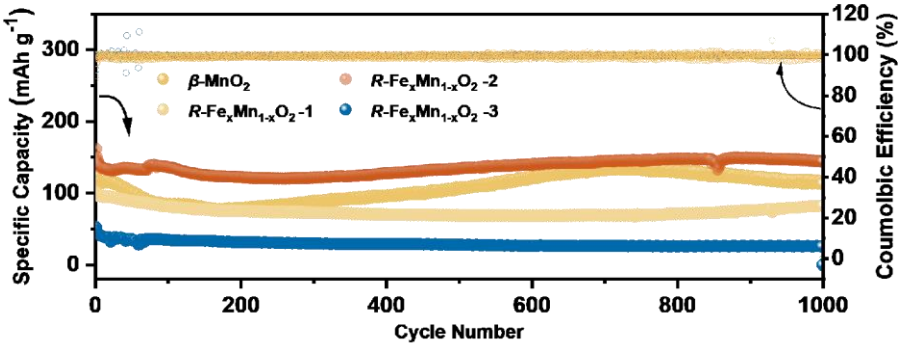


**Supplementary Figure 9.** Cycling performance of four samples at a current density of 1 A $g^{-1}$.

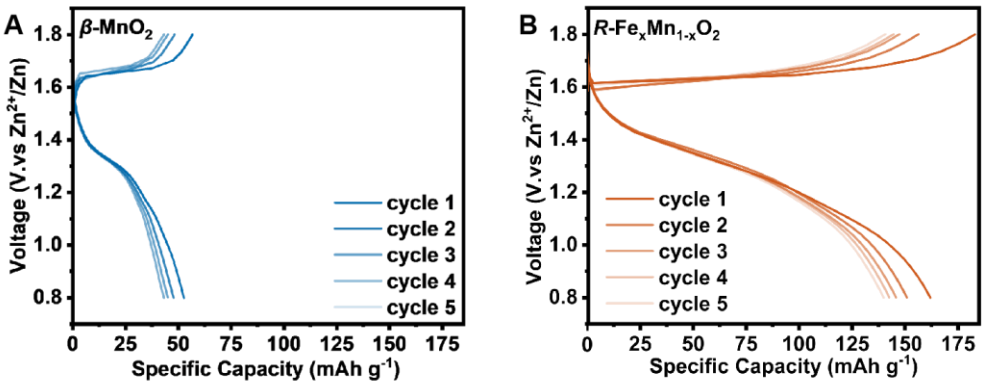


**Supplementary Figure 10.** Charge/discharge curves of $\beta$-$MnO_2$ and $R$-$Fe_xMn_{1-x}O_2$ cathodes at a current density of 1A $g^{-1}$ for the initial five cycles.

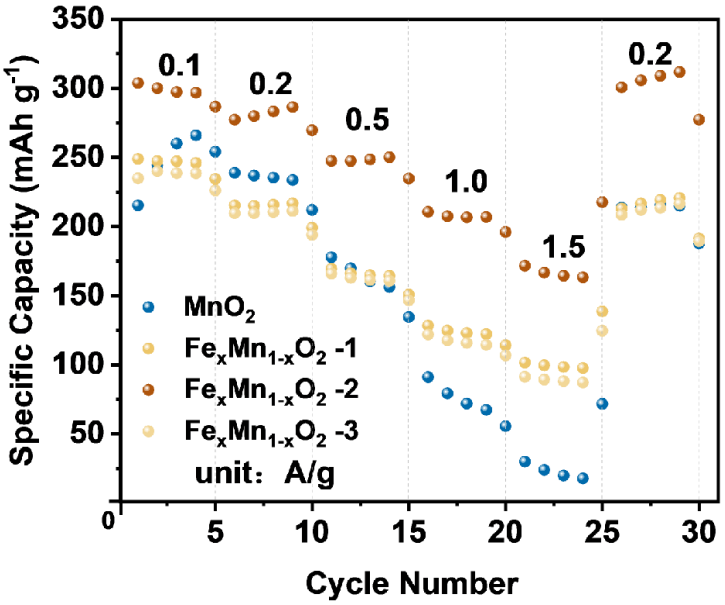


**Supplementary Figure 11.** Rate capabilities of four samples.

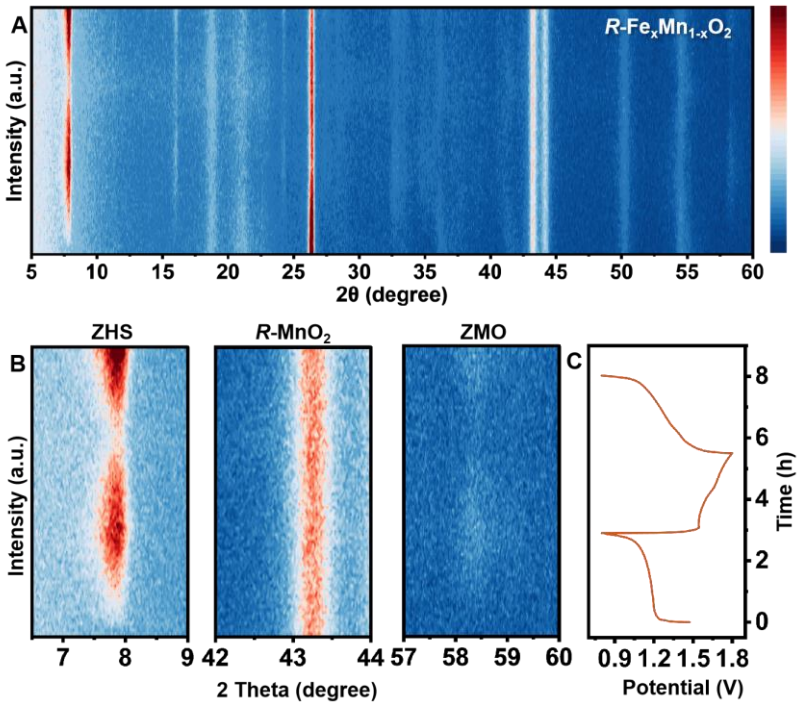


**Supplementary Figure 12.** *in situ* XRD patterns of *R*-$Fe_xMn_{1-x}O_2$ at 0.05 A $g^{-1}$ and the corresponding charge-discharge curves.

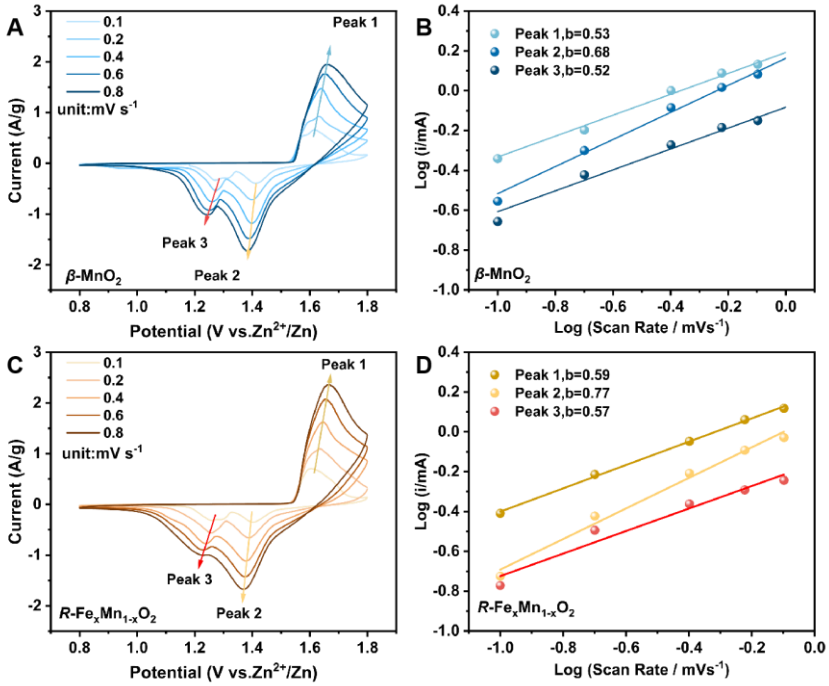


**Supplementary Figure 13.** (A), (C) CV curves of different scan rates of $\beta$-$MnO_2$ and R-$Fe_xMn_{1-x}O_2$ cathodes. (B), (D) b values according to the relationship of log(i) and log(v) at different peaks of $\beta$-$MnO_2$ and *R*-$Fe_xMn_{1-x}O_2$ cathodes.

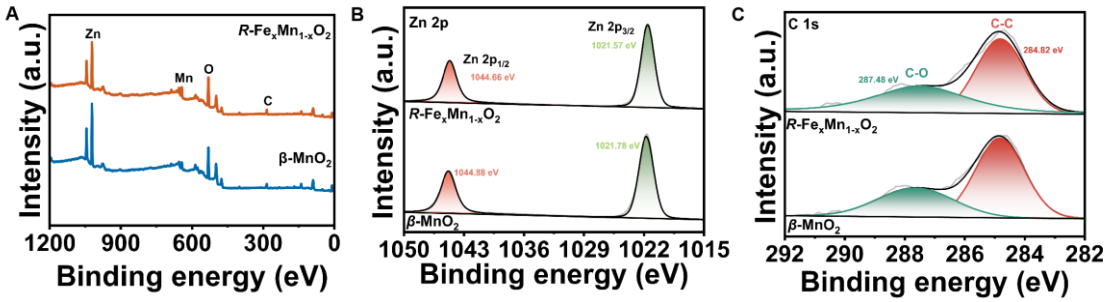


**Supplementary Figure 14.** (A) XPS survey of $\beta$-$MnO_2$ and $R$-$Fe_xMn_{1-x}O_2$ cathodes after 1000 cycles at the current of 1A $g^{-1}$. (B) Zn 2p XPS spectra after cycling. (C) C 1s XPS spectra after cycling.

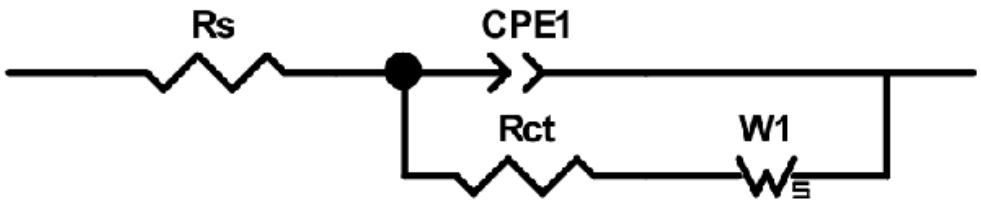


**Supplementary Figure 15.** electrical equivalent circuit served for fitting EIS spectra.

**Supplementary Table 1. Statistics of Mn-based cathode materials electrochemical measurements**

| Cathode materials | Voltage (V) | Reversible capacity (mAh $g^{-1}$) | Current density (A $g^{-1}$) | Cycles | *Ref.* |
|---|---|---|---|---|---|
| CoMn-PBA-DH/PANI | 0.2-1.9 | 97.9 | 0.1 | 1000 | [2] |
| *α*-AMO ($Al^{3+}$ doping) | 0.7-1.9 | 104.2 | 1 | 1000 | [3] |
| $Al_{0.05}$-$MnO_2$ | 0.8-1.8 | 201.8 | 1 | 1000 | [4] |
| CMO@EG | 0.6-1.9 | 115 | 5 | 1000 | [5] |
| Fe-$Mn_3O_4$/C-3 | 0.5-1.8 | 101 | 5 | 800 | [6] |
| *c*-MnHCF | 1.0-2.2 | 73 | 1 | 1000 | [7] |
| Zn//CNT@$MnO_2$ | 0.8-1.8 | 70 | 1 | 90 | [8] |
| Cu-MnO | 1.0-1.8 | 58 | 3 | 1000 | [9] |
| KMO/EG | 1.0-2.0 | 105 | 1 | 500 | [10] |
| $Na_{0.6}MnO_2$ | 1.0-2.0 | 127.2 | 0.2 | 150 | [11] |
| *n*-$Mn_2Mo(CN)_8$/CNTs | 0.3-1.9 | 62 | 2 | 2000 | [12] |
| PrGO–$MnO_x$ | 1.0-1.8 | 76 | 2 | 1500 | [13] |
| *δ*- $MnO_2$ | 0.8-1.9 | 88.9 | 3 | 2000 | [14] |
| $MnO_x$@N-C | 0.8-1.8 | 98 | 2 | 1000 | [15] |
| *α*-KMO | 0.8-1.9 | 99.6 | 1 | 1000 | [16] |
| **_R_-$Fe_xMn_{1-x}O_2$** | **0.8-1.8** | **143.4** | **1** | **1000** | **This work** |

**Supplementary Table 2. Fitting results of *β*-$MnO_2$ and _R_-$Fe_xMn_{1-x}O_2$ from EIS curves**

| | Resistance | $R_s$ (Ω .$cm^2$) | $R_{ct}$ (Ω .$cm^2$) |
|---|---|---|---|
| before | *β*-$MnO_2$ | 2.737 | 197.6 |
| | _R_-$Fe_xMn_{1-x}O_2$ | 9.177 | 112.8 |
| 1000th | *β*-$MnO_2$ | 1.339 | 1720 |
| | _R_-$Fe_xMn_{1-x}O_2$ | 1.723 | 562.9 |

## Reference


[1] J. Zhou, S. Wang, X. Wang, *et al.*, *CrystEngComm*, **2022**, *24*, 7540-7544.

[2] L. Song, S. Ziwei, L. Bingge, *et al.*, *J. Energy Storage*, **2025**, *11*, 15310.

[3] Y. Liu, Z. Jian, Z. Xiaoming, *et al.*, *J. Al. Com.*, **2025**, *1012*, 178502.

[4] Y. Zhao, S. Zhang, Y. Zhang, *et al.*, *Energy Environ. Sci.*, **2023**, *17*, 1279–1290.

[5] P. Guo, G. Yang, C. Wang, *J.Mater. Chem. A*, **2021**, *9*, 16868–16877.

[6] P. Guangxing, W. Zhenyuan, Z. Jichuan, *et al.*, *Energy Technol.*, **2024**, 2401690.

[7] H. Ruo, L. Chen, J. Huang, *et al.*, *Surf. Interf.*, **2024**, *51*, 104594.

[8] Y. Ren, F. Meng, S. Zhang, *et al.*, *Carbon Energy* **2022**, *4*, 446-457.

[9] F. W. Fenta, B. W. Olbasa, M.-C. Tsai, *et al.*, *J. Mater. Chem. A.*, **2020**, *8*, 17595–17607.

[10] H. Changxin, C. Juanjuan, O. Yun, *et al.*, *J. Electroanal. Chem.*, **2024**, *975*, 118732.

[11] A. Williams, P. K. Nayak, *Mater. Adv.*, **2024**, *5*, 9699-9715.

[12] P. Jinrui, X. Yutao, J. Zhenyuan, *et al.*, *J. Colloid Interf. Sci.*, **2025**, *686*, 27-36.

[13] Z.-Q. Wang, X.-D. Liu, H.-M. Chen, *et al.*, *J.Mater. Chem. A*, **2022**, *11*, 1380–1393.

[14] F. Wan, R. Liu, Y. Xia, *et al.*, *Inorg. Chem.* **2024**, *63*, 6988-6997.

[15] F. Yanqing, W. Qiliang, Z.Gaixia, *Adv. Energy Mater.*, **2018**, *11*, 1380–1393.

[16] Q. Yang, Y. Chen, Y. Yang, *et al.*, *Ind. Eng. Chem. Res.*, **2023**, *62*, 16757-16765.